LETTERS

CONVECTIVE LOSSES DURING CURRENT INITIATION IN TOKAMAKS

M. VALOVIČ (Institute of Plasma Physics, Czechoslovak Academy of Sciences, Prague, Czechoslovakia)

ABSTRACT. The mechanism of convective losses in the phase preceding the formation of rotational transform is studied on the CASTOR tokamak. It is shown that convection is caused by $\vec{E} \times \vec{B}$ drift associated with a strong perpendicular electrostatic field. This field is generated by charge separation as a result of a directed flow of electrons along non-toroidal magnetic field lines intersecting the wall. Convection exceeds Bohm diffusion by a factor of 700 for a perpendicular magnetic field of 10^{-3} T.

1. INTRODUCTION

Two important problems in connection with the design of a tokamak reactor are the ionization of neutral gas and the initiation of the plasma current. It is known that the inductive voltage must be sufficiently high during plasma breakdown to overcome the barrier of poor plasma confinement. A rough extrapolation from existing tokamaks led to the prediction of a minimum breakdown voltage of 100 V for INTOR [1]. This voltage, however, cannot be induced by a superconducting Ohmic heating coil. Therefore, an alternative breakdown scheme which uses an additional copper solenoid has been proposed for INTOR [2]. Also radio-frequency assisted breakdown has been included in this project [3]. Furthermore, it has been shown that the breakdown voltage can be considerably reduced by careful treatment of such parameters as the cleaning conditions, the filling atom density and the rate of rise of the loop voltage. Even on the JET tokamak, a breakdown voltage of less than 20 V without preionization is sufficient [4].

The most important factor determining the breakdown voltage is the level of convective losses during the phase in which rotational transform is not yet established. The mechanism of this convection is not yet fully understood. Studies of electron drift due to field gradients and centrifugal forces have been reported in Refs [5–8]. However, these loss models are not consistent with the condition of plasma quasi-neutrality.

Ambipolar convection in the absence of toroidal current and with zero perpendicular magnetic field has been considered theoretically [9, 10]. In these investigations, the convective losses are caused by $\vec{E} \times \vec{B}$ drift due to the plasma electrostatic field. In a tokamak, however, perpendicular magnetic fields are always present because of eddy currents in the conducting parts of the machine. Particularly under routine operating conditions of a reactor, relatively high perpendicular magnetic fields must be expected (0.01 T for INTOR). Ambipolar losses with a perpendicular magnetic field were studied experimentally by Nakao et al. [11]. In this case the plasma potential was found to have a thermal value.

In contrast to these findings, the toroidal current is not zero during the formation of rotational transform in a tokamak. A directed flow of electrons can considerably change the plasma potential and thus the character of the convection. In the present paper it is shown that such an effect actually takes place.

The dependence of the plasma potential on the perpendicular magnetic field has been studied by Schüller et al. [12]. However, in this experiment rotational transform was established and the plasma was fully ionized.

2. EXPERIMENTAL SET-UP

The experiment was carried out on the CASTOR tokamak, which has a major radius R_0 of 0.4 m. The cross-section of the stainless steel liner has a radius of 0.1 m. The plasma minor radius, a = 85 mm, is determined by four molybdenum limiters. The aperture limiter consists of two C-shaped segments separated by a vertical gap. Two rail limiters are placed at the upper and lower sides of the aperture. All segments are isolated from one another and from the liner. The plasma is shielded (except at six diagnostic ports) by a copper shell.

During the experiment, the hydrogen atom filling density had a constant value of $n = 2.5 \times 10^{19}$ m^{-3}. The neutral gas was preionized by an electron gun. The toroidal magnetic field was $B_T = 1.3$ T. The loop voltage was induced through an iron core transformer by discharging one condenser into the primary windings. The rate of rise of the loop voltage, dU_L/dt, was kept at 8×10^4 V·s^{-1}.

Variation of the vertical (B_V) and horizontal (B_H) magnetic fields was in the range 0–2.5 mT. Their orientation was such that $B_H \geqslant 0$ and $B_V \leqslant 0$, with (R, z) denoting a cylindrical co-ordinate system with the z-axis oriented upwards. The inhomogeneity of these magnetic fields in the plasma cross-section was 30%.

Net plasma current was detected by a Rogowski coil located in the limiter shadow. The position of the current channel was determined by Mirnov coils. As long as rotational transform and consequently Shafranov equilibrium are not established, standard positional measurements cannot be made. Therefore the plasma is treated as a thin toroidal wire in an ideal shielding. This treatment, however, leads to incorrect plasma positions in subsequent phases. Floating potential, electron density and temperature were measured by a set of Langmuir probes. The probes were located in one cross-section and were placed along the plasma edge at points $R = R_0 \pm a$, $z = 0$, and $R = R_0$, $z = \pm a$. One probe could be moved in the vertical direction. The toroidal angle between the probes and the limiters was 45°.

3. RESULTS

The dynamics of plasma breakdown are shown in Fig. 1. The loop voltage U_L rises until the breakdown voltage U_B is reached. U_B is minimum for the horizontal and vertical magnetic fields when $B_H^{OPT} = 0.63$ mT and $B_V^{OPT} = -0.73$ mT. If the total magnetic field is defined as

$$\vec{B}_\perp = (B_H, B_V) - (B_H^{OPT}, B_V^{OPT})$$

then, for $|B_\perp| = 0 - 2$ mT, the breakdown voltage varies from 20 V to 36 V. The magnetic field $(-B_H^{OPT}, -B_V^{OPT})$ represents the sum of fields generated by a variety of currents: the primary current, liner and plasma currents, and image currents in the iron core and copper shell.

The Rogowski coil detects the plasma current I_p, starting from a detection level of 0.1 A. The current rises exponentially by three orders of magnitude until it reaches a certain value; this is the breakdown current I_B (Fig. 1). The loop voltage does not change much during this exponential phase. The difference between the loop voltage and the surface voltage is also small. Therefore the toroidal electric field is approximately uniform during this time interval, i.e. $E = U_B/2\pi R_0$. The reduced electric field E/n determines the electron drift velocity v_D, the electron temperature T_e and the exponential rate of rise of the lossless avalanche beta [13–15]. For $U_B = 20$–36 V, these parameters are: $v_D = (0.9\text{–}1.3) \times 10^6$ m·s^{-1}, $T_e \approx 10$ eV and $\beta = (0.95\text{–}1.5) \times 10^5$ s^{-1}.

The exponential rise of the plasma current indicates that I_p is proportional to the electron density. It also implies that the ratio of lost electrons to born electrons, $\lambda = 1 - \gamma/\beta$, is constant during this time interval. Here, γ denotes the rate $d(\ln I_p)/dt$. Figure 2 shows that λ is proportional to the total perpendicular magnetic field and reaches a value higher than 0.5.

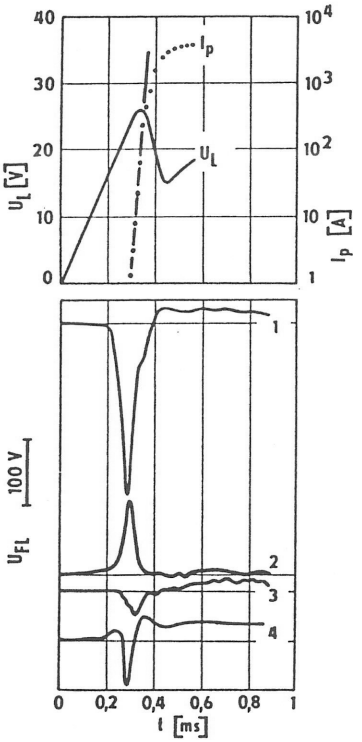

FIG. 1. Temporal evolution of loop voltage U_L, plasma current I_p and floating potential U_{FL} of the probes for external magnetic fields: $B_H = 0.63$ mT, $B_V = -1.8$ mT. Numbers 1, 2, 3 and 4 denote the probe positions: $(R, z) = (R_0, a)$, $(R, z) = (R_0, -a)$, $(R, z) = (R_0 + a, 0)$ and $(R, z) = (R_0 - a, 0)$, respectively. (In the text, these are referred to as upper, lower, outer and inner probes.)

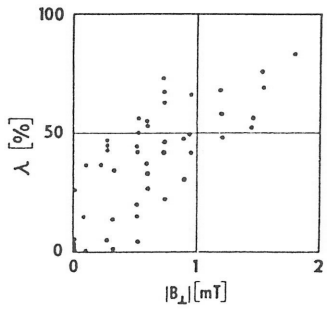

FIG. 2. Dependence of the loss ratio λ on the absolute value of the total perpendicular magnetic field.

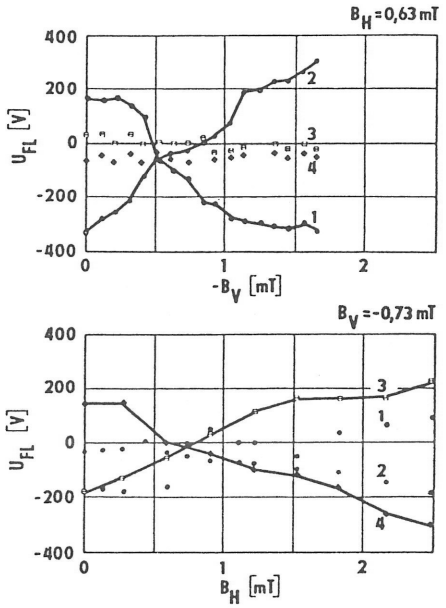

FIG. 3. Dependence of the floating potential of the probes at breakdown on the vertical and horizontal magnetic fields. The probe positions denoted by numbers 1–4 are the same as in Fig. 1.

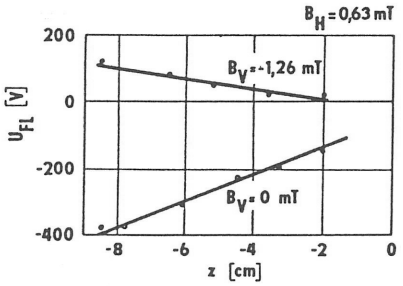

FIG. 4. Vertical profile of the floating potential of the probes at breakdown for two values of the vertical magnetic field.

The value of the plasma current at the end of the exponential phase, I_B, depends weakly on $|B_\perp|$ and is approximately 400 A. The corresponding electron density is $n_B = I_B/e\pi\, a^2 v_D \approx 2 \times 10^{17}$ m^{-3} (e is the electron charge). At this time, Coulomb collisions begin to prevail and the electrons feel the enhancement of the collision cross-section in the factor $\ln \Lambda \approx 11$ (Coulomb logarithm). This leads to relaxation of the longitudinal electron energy. The probe characteristics show an evolution from a non-Maxwellian distribution function with a characteristic longitudinal energy of 40 eV at the end of the avalanche to a Maxwellian distribution function with a temperature of 15 eV 0.3 ms after this end-point.

The evolution of the electrostatic field in the plasma is deduced from the floating potential of the probes relative to the liner. In Fig. 1 it can be seen that the floating potentials exhibit sharp extremes at breakdown and then relax. This relaxation is due to the poloidal mixing of the space charge after formation of rotational transform.

The peak values of the floating potentials U_{FL} depend markedly on the perpendicular magnetic field. As shown in Fig. 3, a change of the vertical magnetic field changes the floating potentials of the upper and lower probes while those of the inner and outer probes remain approximately constant. If the horizontal magnetic field is changed, the floating potentials of the inner and outer probes also change. This dependence on the magnetic field is also true for the floating potentials of the limiter segments. The maximum difference between the floating potential of the probe and that of a correspondingly placed segment is 15% of U_{FL}.

Figure 4 shows the results of measurements of the vertical profile of the floating potential at breakdown. If the total perpendicular magnetic field is sufficiently large, U_{FL} has a linear profile in the direction of $\vec{B}_\perp$. For small $|B_\perp|$, the floating potentials have a complicated temporal evolution and space profile (not shown in Fig. 4). This is because the stray magnetic fields are time dependent while the external magnetic fields are constant. A further reason for this is the fact that the profiles of the stray magnetic fields are quite different and therefore it is impossible to perfectly compensate stray fields throughout the whole plasma volume even at one particular instant. The optimum configuration to be realized is that in which the perpendicular field has different orientations in various parts of the plasma cross-section.

4. DISCUSSION

The behaviour of the floating potentials of probes at breakdown indicates that the electrostatic field is caused by the plasma polarization and not by electron deficiency. Since the profile of U_{FL} is linear, the electrostatic field is homogeneous and therefore the charges are to the limiter shadow. This configuration is formed by a shift of the electrons relative to the ions when the density profile has a considerable gradient only in the limiter shadow and is flat elsewhere.

For $|B_\perp| \gtrsim 1$ mT, the floating potential of a probe is large compared with the potential of the sheath

around the probe. The difference between the floating potentials of opposite probes thus gives the potential difference over the plasma cross-section: $2a\,E_\perp$. When the vertical and horizontal orientations of the magnetic field from Fig. 3 are summed up, the perpendicular electrostatic field of the plasma is

$$\vec{E}_\perp \approx -5 \times 10^6\, \vec{B}_\perp \qquad (1)$$

in units of $V \cdot m^{-1}$ and T. Such a field is strongly suprathermal: $eE_\perp\, a \approx 60\, T_e$ for $B_\perp = 1$ mT.

It is obvious that only the electrons are responsible for the polarization of the plasma. The longitudinal mobility of the ions in the electric field is low. The toroidal drift is negligible because of the low ion temperature.

The electron component moves transversely owing to two drifts: the toroidal drift with a velocity $T_e/eB_T R_0 \approx 20\ m \cdot s^{-1}$ and the drift along the lines of force of the magnetic field with a velocity $v_\perp = v_D B_\perp / B_T \approx 1000\ m \cdot s^{-1}$. Note that during the avalanche the electron thermal velocity is approximately $2v_D$. The horizontal polarization is caused only by directed flow along the lines of force. The vertical polarization can be attributed to the two drifts. However, since the configurations of the two orientations are similar, we conclude that flow along the lines of force also dominates in the vertical direction.

This conclusion can be used to explain qualitatively the orientation and the high value of the perpendicular electrostatic field. The maximum possible value of $E_\perp$ is given by the condition that the projection of the electric field along the lines of force vanish ($v_D = 0$):

$$\vec{E}_\perp = -E \frac{B_T}{|B_\perp|^2} \cdot \vec{B}_\perp \qquad (2)$$

In the experiment, the perpendicular electrostatic field is indeed antiparallel to $\vec{B}_\perp$. Its value ($E_\perp = 5000\ V \cdot m^{-1}$ for $B_\perp = 1$ mT) is one-half of that given by Eq. (2). Since the time-scale for buildup of the electrostatic field (1 ns) is much shorter than γ^{-1}, the limitation of the field to below its upper limit (2) is not caused by the non-stationarity of the electron density. Therefore the transverse electron current, $I_\perp = 2\pi\, R_0\, 2a\, en_B v_\perp \approx 16$ A, must be counter-balanced by a current flowing through the limiter shadow and/or through the liner. In the limiter shadow, the plasma is non-neutral and $\vec{E}_\perp$ is normal to the liner. Thus a current can be driven by an $\vec{E} \times \vec{B}$ drift along the wall. However, this current is not able to compensate $I_\perp$. A sufficiently large current through the liner can be closed by photoemission and by the acceleration of ions due to the large electric field near the wall. Note that secondary electron emission is negligible. However, a detailed theory is needed to determine the liner current and thus to find the actual value of $E_\perp$. The situation just described does not hold for small magnetic fields, $|B_\perp| \lesssim 0.5$ mT, when $\vec{B}_\perp$ and consequently $\vec{E}_\perp$ are strongly inhomogeneous.

As reported in Ref. [12], a vertical polarization of the plasma was caused by its R-oriented velocity $\vec{u}$, as a combined effect of the plasma pressure and the unmatched vertical equilibrium field. If $I_\perp = 0$, Ohm's law gives $\vec{E}_\perp = -\vec{u} \times \vec{B}_\perp$ in this situation. However, in our case, such a mechanism cannot explain plasma polarization. This follows from the fact that the term in the MHD force which can drive the plasma in both the vertical direction and the horizontal direction, $\vec{I} \times \vec{B}$, is zero because the current flows along the field lines during the avalanche.

The losses are caused by the $\vec{E} \times \vec{B}$ movement of the plasma towards the limiter shadow and by a subsequent plasma flow on the limiter with ion sound

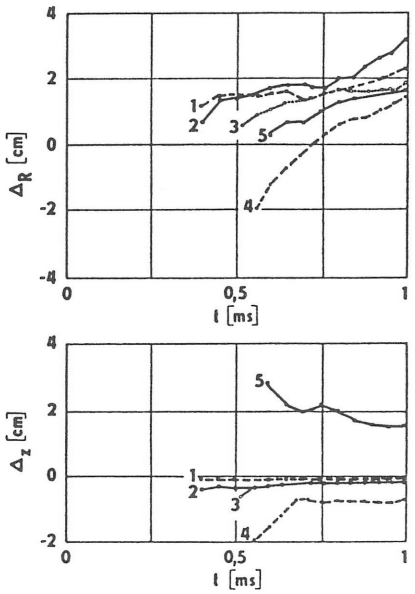

FIG. 5. Horizontal displacement, $\Delta_R = R - R_0$, and vertical displacement, $\Delta_z = z$, of the current channel for different values of the corrected perpendicular magnetic field $\vec{B}_\perp$. Trace 1 refers to $\vec{B}_\perp = (0, 0)$ mT. Traces 3, 5 (Δ_z shift) refer to $\vec{B}_\perp = (-0.63, 0)$ mT and (1.87, 0) mT; and traces 4, 2 (Δ_R shift) refer to $\vec{B}_\perp = (0, -0.95)$ mT and (0, 0.73) mT.

velocity. An estimate of the characteristic loss time for $B_\perp = 1$ mT gives

$$\tau \approx \frac{B_\perp a}{E_\perp} \approx 2 \times 10^{-5} \text{ s}$$

This value is 700 times lower than the value of the loss time determined from Bohm diffusion and is approximately equal to the value given by the exponential rate $(\lambda\beta)^{-1} \approx 2 \times 10^{-5}$ s. Therefore, it seems that the observed γ-rate is determined by convective losses. This statement is not trivial because γ can be affected by a reverse effect of $E_\perp$ which reduces E/n along the lines of force of the magnetic field.

The characteristic times of the losses and of the ionization are comparable. This leads to the eccentric density profile at the end of the avalanches. Figure 5 shows the evolution of the position of the current channel for different values of $\vec{B}_\perp$. The traces shown begin at breakdown. When $B_\perp = 0$, a current channel forms close to the centre. When $|B_\perp| \gtrsim 1$ mT, the eccentricity is approximately 0.4a and the displacement of the plasma at breakdown follows the orientation of the $\vec{E} \times \vec{B}$ drift.

5. CONCLUSIONS

In summary, it can be said that the presence of perpendicular magnetic fields during the formation of rotational transform in a tokamak results in strong polarization of the plasma. The associated $\vec{E} \times \vec{B}$ drift of the current exceeds the Bohm diffusion by two to three orders of magnitude. Note that this effect will also take place in the case of RF startup scenarios.

ACKNOWLEDGEMENTS

The author would like to thank V. Kopecký for his support, and J. Badalec, K. Jakubka, J. Stöckel and F. Žáček for their help.

The author is grateful to the referee for directing his attention to the work of Schüller et al. [12] and for valuable criticism especially concerning the counter-balancing current.

REFERENCES

[1] INTOR GROUP, International Tokamak Reactor: Zero Phase (Rep. Int. Workshop Vienna, 1979), IAEA, Vienna (1980).
[2] INTOR GROUP, International Tokamak Reactor: Phase One (Rep. Int. Workshop Vienna, 1980 and 1981), IAEA, Vienna (1982).
[3] INTOR GROUP, International Tokamak Reactor: Phase Two A, Part I (Rep. Int. Workshop Vienna, 1981–1983), IAEA, Vienna (1983).
[4] TANGA, A., THOMAS, P.R., CORDEY, J.G., CHRISTIANSEN, J.P., EJIMA, S., et al., Start-up of the Ohmic Phase in JET, Rep. JET-P(85)23, JET Joint Undertaking, Abingdon, Oxfordshire (1985).
[5] PAPOULAR, R., Nucl. Fusion **16** (1976) 37.
[6] PRINZLER, H., HEYMANN, P., STÖCKEL, J., BADALEC, J., ŽÁČEK, F., JAKUBKA, K., KOPECKÝ, V., Czech, J. Phys., B **34** (1984) 665.
[7] PENG, M., BOROVSKI, S.K., KAMMASH, T., Nucl. Fusion **18** (1978) 1489.
[8] CARRETTA, U., FARINA, D., LONTANO, M., MAROLI, C., MINARDI, E., PETRILLO, V., POZZOLI, R., in Plasma Physics and Controlled Nuclear Fusion Research 1984 (Proc. 10th Int. Conf. London, 1984), Vol. 3, IAEA, Vienna (1985) 279.
[9] ABRAMOV, V.A., POGUTSE, O.P., YURCHENKO, E.I., Fiz. Plazmy **1** (1975) 536.
[10] BULYGINSKIJ, D.G., YUFEREV, V.S., GALAKTINOV, E.V., Fiz. Plazmy **3** (1977) 963.
[11] NAKAO, S., OGURA, K., TERUMICHI, Y., TANAKA, S., Phys. Lett., A **96** (1983) 405.
[12] SCHÜLLER, F.C., DE HAAS, R.S., BRANDT, B., SCHRADER, W.J., ORNSTEIN, L.Th.M., BRAAMS, C.M., in Plasma Physics and Controlled Nuclear Fusion Research 1974 (Proc. 5th Int. Conf. Tokyo, 1974), Vol. 2, IAEA, Vienna (1975) 725.
[13] SCHLUMBOHM, H, Z. Phys. **182** (1965) 317.
[14] VARNERIN, L.J., BROWN, S.C., Phys. Rev. **79** (1950) 946.
[15] BUFFA, A., MALESANI, G., NALESSO, G.F., Phys. Rev., A **3** (1971) 95.

(Manuscript received 10 March 1986
Final manuscript received 27 October 1986)